



High energy passively Q-switched Er-doped fiber laser based on $\text{Mo}_{0.5}\text{W}_{0.5}\text{S}_2$ saturable absorber

JUNLI WANG,^{1,*} CHENXI DOU,¹ LEI CHEN,¹ HAITING YAN,² LINGJIE MENG,² JIANGFENG ZHU,¹ AND ZHIYI WEI³

¹School of Physics and Optoelectronic Engineering, Xidian University, Xi'an 710071, China

²School of Science, Xi'an Jiaotong University, Xi'an 710049, China

³Beijing National Laboratory for Condensed Matter Physics, Institute of Physics, Chinese Academy of Sciences, Beijing 100190, China

*dispersion@126.com

Abstract: A passively Q-switched Er-doped fiber laser based on a novel transition metal sulfide (TMDs) $\text{Mo}_{0.5}\text{W}_{0.5}\text{S}_2$ absorber is reported for the first time. There are two different types of $\text{Mo}_{0.5}\text{W}_{0.5}\text{S}_2$ -based saturable absorbers (SAs) that achieve Q-switching operation, one of which is depositing the $\text{Mo}_{0.5}\text{W}_{0.5}\text{S}_2$ on the surface of the tapered fiber, and the maximum single pulse energy of 172.91 nJ and minimum pulse width of 1.42 μs is obtained. While the other is transferring $\text{Mo}_{0.5}\text{W}_{0.5}\text{S}_2$ -PVA (polyvinyl alcohol: PVA) SA film onto a standard FC/APC fiber end face, the high single pulse energy of 246.5 nJ and the minimum pulse width is 1.92 μs is obtained, and the modulation depth of SAs detected by the twin-detector method is 15%. The experiment results show that $\text{Mo}_{0.5}\text{W}_{0.5}\text{S}_2$ can be considered as a promising candidate for pulse fiber laser applications and other photoelectric devices.

© 2018 Optical Society of America under the terms of the [OSA Open Access Publishing Agreement](#)

OCIS codes: (140.3540) Lasers, Q-switched; (140.3500) Lasers, erbium; (160.4236) Nanomaterials.

References and links

1. Q. Bao, H. Zhang, Y. Wang, Z. Ni, Y. Yan, Z. Shen, K. Loh, and D. Tang, "Atomic-Layer Graphene as a Saturable Absorber for Ultrafast Pulsed Lasers," *Adv. Funct. Mater.* **19**(19), 3077–3083 (2009).
2. Z. Sun, T. Hasan, F. Torrisi, D. Popa, G. Privitera, F. Wang, F. Bonaccorso, D. M. Basko, and A. C. Ferrari, "Graphene mode-locked ultrafast laser," *ACS Nano* **4**(2), 803–810 (2010).
3. S. Y. Choi, H. Jeong, B. H. Hong, F. Rotermund, and D. I. Yeom, "All-fiber dissipative soliton laser with 10.2 nJ pulse energy using an evanescent field interaction with graphene saturable absorber," *Laser Phys. Lett.* **11**(1), 015101 (2014).
4. C. Zhao, H. Zhang, X. Qi, Y. Chen, Z. Wang, S. Wen, and D. Tang, "Ultra-short pulse generation by a topological insulator based saturable absorber," *Appl. Phys. Lett.* **101**(21), 118 (2012).
5. Y. Chen, C. Zhao, H. Huang, S. Chen, P. Tang, Z. Wang, S. Lu, H. Zhang, S. Wen, and D. Tang, "Self-Assembled Topological Insulator: Bi_2Se_3 Membrane as a Passive Q-Switcher in an Erbium-Doped Fiber Laser," *J. Lightwave Technol.* **31**(17), 2857–2863 (2013).
6. P. Tang, X. Zhang, C. Zhao, Y. Wang, H. Zhang, D. Shen, S. Wen, D. Tang, and D. Fan, "Topological Insulator: Saturable Absorber for the Passive Q-Switching Operation of an in-Band Pumped 1645-nm Er:YAG Ceramic Laser," *IEEE Photonics J.* **5**(2), 1500707 (2013).
7. Y. Chen, G. Jiang, S. Chen, Z. Guo, X. Yu, C. Zhao, H. Zhang, Q. Bao, S. Wen, D. Tang, and D. Fan, "Mechanically exfoliated black phosphorus as a new saturable absorber for both Q-switching and Mode-locking laser operation," *Opt. Express* **23**(10), 12823–12833 (2015).
8. Z. C. Luo, M. Liu, Z. N. Guo, X. F. Jiang, A. P. Luo, C. J. Zhao, X. F. Yu, W. C. Xu, and H. Zhang, "Microfiber-based few-layer black phosphorus saturable absorber for ultra-fast fiber laser," *Opt. Express* **23**(15), 20030–20039 (2015).
9. K. Park, J. Lee, Y. Lee, W. Choi, J. Lee, and Y. Song, "Black phosphorus saturable absorber for ultrafast mode-locked pulse laser via evanescent field interaction," *Ann. Phys.* **527**(11–12), 770–776 (2016).
10. H. Zhang, S. B. Lu, J. Zheng, J. Du, S. C. Wen, D. Y. Tang, and K. P. Loh, "Molybdenum disulfide (MoS_2) as a broadband saturable absorber for ultra-fast photonics," *Opt. Express* **22**(6), 7249–7260 (2014).
11. D. Mao, Y. Wang, C. Ma, L. Han, B. Jiang, X. Gan, S. Hua, W. Zhang, T. Mei, and J. Zhao, " WS_2 mode-locked ultrafast fiber laser," *Sci. Rep.* **5**(7965), 7965 (2015).
12. H. Liu, A. P. Luo, F. Z. Wang, R. Tang, M. Liu, Z. C. Luo, W. C. Xu, C. J. Zhao, and H. Zhang, "Femtosecond pulse erbium-doped fiber laser by a few-layer MoS_2 saturable absorber," *Opt. Lett.* **39**(15), 4591–4594 (2014).

13. S. Bikorimana, P. Lama, A. Walser, R. Dorsinville, S. Anghel, A. Mitioglu, A. Micu, and L. Kulyuk, "Nonlinear optical responses in two-dimensional transition metal dichalcogenide multilayer: WS₂, WSe₂, MoS₂ and Mo_{0.5}W_{0.5}S₂," *Opt. Express* **24**(18), 20685 (2016).
14. W. S. Yun, S. W. Han, S. C. Hong, I. G. Kim, and J. D. Lee, "Thickness and strain effects on electronic structures of transition metal dichalcogenides: 2H-MX₂ semiconductors (M = Mo, W; X = S, Se, Te)," *Phys. Rev. B Condens. Matter* **85**(3), 033305 (2006).
15. A. Kuc, N. Zibouche, and T. Heine, "Influence of quantum confinement on the electronic structure of the transition metal sulfide TS₂," *Phys. Rev. B Condens. Matter* **83**(24), 2237–2249 (2011).
16. A. V. Krivosheeva, V. L. Shaposhnikov, R. G. Khameneh, V. E. Borisenko, and J. L. Lazzari, "Electronic and optical properties of two-dimensional MoS₂, WS₂, and Mo_{0.5}W_{0.5}S₂ from first-principles," *Physics, Chemistry and Applications of Nanostructures* **2015**, 32–35 (2015).
17. L. Kou, T. Frauenheim, and C. Chen, "Nanoscale Multilayer Transition-Metal Dichalcogenide Heterostructures: Band Gap Modulation by Interfacial Strain and Spontaneous Polarization," *J. Phys. Chem. Lett.* **4**(10), 1730–1736 (2013).
18. Z. Yin, H. Li, H. Li, L. Jiang, Y. Shi, Y. Sun, G. Lu, Q. Zhang, X. Chen, and H. Zhang, "Single-layer MoS₂ phototransistors," *ACS Nano* **6**(1), 74–80 (2012).
19. Y. Chen, J. Xi, D. O. Dumcenco, Z. Liu, K. Suenaga, D. Wang, Z. Shuai, Y. S. Huang, and L. Xie, "Tunable band gap photoluminescence from atomically thin transition-metal dichalcogenide alloys," *ACS Nano* **7**(5), 4610–4616 (2013).
20. J. Li, G. Mo, Y. Bai, and A. Bao, "Microwave-assisted hydrothermal synthesis and luminescence of NaEu(MoO₄)₂:Sm³⁺ powders," *J. Mater. Sci. Mater. Electron.* **26**(10), 7390–7396 (2015).
21. F. Bilodeau, K. O. Hill, S. Faucher, and D. C. Johnson, "Low-loss highly overcoupled fused couplers: Fabrication and sensitivity to external pressure," *J. Lightwave Technol.* **6**(10), 1476–1482 (1988).
22. H. Li, H. Xia, C. Lan, C. Li, X. Zhang, J. Li, and Y. Liu, "Passively Switched Erbium-Doped Fiber Laser Based on Few-Layer MoS₂ Saturable Absorber," *IEEE Photonics Technol. Lett.* **27**(1), 69–72 (2014).
23. W. Liu, L. Pang, H. Han, K. Bi, M. Lei, and Z. Wei, "Tungsten disulphide for ultrashort pulse generation in all-fiber lasers," *Nanoscale* **9**(18), 5806–5811 (2017).
24. Z. Yu, Y. Song, J. Tian, Z. Dou, H. Guoyu, K. Li, H. Li, and X. Zhang, "High-repetition-rate Q-switched fiber laser with high quality topological insulator Bi₂Se₃ film," *Opt. Express* **22**(10), 11508–11515 (2014).
25. H. Li, H. Xia, C. Lan, C. Li, X. Zhang, J. Li, and Y. Liu, "Passively, Q-Switched Erbium-Doped Fiber Laser Based on Few-Layer MoS₂ Saturable Absorber," *IEEE Photonics Technol. Lett.* **27**(1), 69–72 (2014).
26. J. Ren, S. Wang, Z. Cheng, H. Yu, H. Zhang, Y. Chen, L. Mei, and P. Wang, "Passively Q-switched nanosecond erbium-doped fiber laser with MoS₂ saturable absorber," *Opt. Express* **23**(5), 5607–5613 (2015).
27. H. Xia, H. Li, C. Lan, C. Li, J. Du, S. Zhang, and Y. Liu, "Few-layer MoS₂ grown by chemical vapor deposition as a passive Q-switcher for tunable erbium-doped fiber lasers," *Photon. Res.* **3**(3), A92 (2015).
28. B. Chen, X. Zhang, K. Wu, H. Wang, J. Wang, and J. Chen, "Q-switched fiber laser based on transition metal dichalcogenides MoS₂, MoSe₂, WS₂, and WSe₂," *Opt. Express* **23**(20), 26723–26737 (2015).
29. S. H. Kassani, R. Khazaeinezhad, H. Jeong, T. Nazari, D. I. Yeom, and K. Oh, "All-fiber Er-doped Q-Switched laser based on Tungsten Disulfide saturable absorber," *Opt. Mater. Express* **5**(2), 373–379 (2015).
30. R. Khazaeinezhad, T. Nazari, H. Jeong, K. Park, B. Kim, D. I. Yeom, and K. Oh, "Passive Q-Switching of an All-Fiber Laser Using WS₂-Deposited Optical Fiber Taper," *IEEE Photonics J.* **7**(5), 1–7 (2015).
31. M. Zhang, G. Hu, G. Hu, R. C. T. Howe, L. Chen, Z. Zheng, and T. Hasan, "Yb- and Er-doped fiber laser Q-switched with an optically uniform, broadband WS₂ saturable absorber," *Sci. Rep.* **5**(1), 17482 (2015).
32. R. Wei, H. Zhang, X. Tian, T. Qiao, Z. Hu, Z. Chen, X. He, Y. Yu, and J. Qiu, "MoS₂ nanoflowers as high performance saturable absorbers for an all-fiber passively Q-switched erbium-doped fiber laser," *Nanoscale* **8**(14), 7704–7710 (2016).
33. H. Chen, Y. Chen, J. Yin, X. Zhang, T. Guo, and P. Yan, "High-damage-resistant tungsten disulfide saturable absorber mirror for passively Q-switched fiber laser," *Opt. Express* **24**(15), 16287–16296 (2016).
34. L. Li, Y. Wang, Z. F. Wang, X. Wang, and G. Yang, "High energy Er-doped Q-switched fiber laser with WS₂ saturable absorber," *Opt. Commun.* **406**, 80 (2017).
35. B. Guo, Y. Yao, P. G. Yan, K. Xu, J. Liu, S. Wang, and Y. Li, "Dual-Wavelength Soliton Mode-Locked Fiber Laser with a WS₂-Based Fiber Taper," *IEEE Photonics Technol. Lett.* **28**(3), 323–326 (2016).

1. Introduction

In recent years, a variety of two dimensional(2D) materials such as graphene [1–3], topological insulator(TI) [4–6] and black phosphorus(BP) [7–9] has attracted great attention due to their excellent photoelectric and thermal properties, which can be used as a saturable absorber (SA) to achieve high pulse energy and short pulse duration in Q-switching or mode-locking system. Among those 2D nonlinear optical materials, graphene is more desirable due to its ultra-broad absorption bandwidth and fast saturable recovery time, but it is hard to create an optical bandgap to fit a certain wavelength range. Beyond graphene, different kinds of synthetic TMDs [10–12] such as molybdenum disulphide(MoS₂), tungsten

disulphide(WS_2) as well as a new mixed molybdenum tungsten disulphide($\text{Mo}_{1-x}\text{W}_x\text{S}_2$) have considerable potential as an emerging generation of photonic nanomaterials because of their unique optical, mechanical and electronic characteristics [13]. The TMDs are expressed as MX_2 ($\text{M} = \text{Mo}, \text{W}, \dots$), M is a transition metal and X is a chalcogen. The two layers of sulfur atoms are interspersed with a layer of metal atoms, which is similar to the structure of sandwich [14]. In the previous reports, monolayer TMDs possess a direct band gap while multilayer and bulk state one possess an indirect band gap [15]. In 2013, It has been reported that substitution of W atoms by Mo atoms can produce a new compound $\text{Mo}_{1-x}\text{W}_x\text{S}_2$ with the structure and fingerprint of principle optical features of WS_2 and MoS_2 [16]. In this work, it is presented that bulk state MoS_2 and WS_2 have the gaps of 1.24 eV and 1.31 eV, double layer can increased the gap to 1.40 eV and 1.57 eV. Whereas bulk state and double layer $\text{Mo}_{0.5}\text{W}_{0.5}\text{S}_2$ possesses the gaps of 1.14 eV and 1.29 eV, respectively. These indicates that $\text{Mo}_{0.5}\text{W}_{0.5}\text{S}_2$ has a wider absorption bandwidth. And those TMDs are layer-depended materials, in which band gap increases with the decrease of the number of layer [17]. This property of tunable band gap engineering is of great importance for some electronic and optoelectronic applications [18]. Thus, alloying TMD of $\text{Mo}_{1-x}\text{W}_x\text{S}_2$ has been proposed by theoretical calculations [16] and demonstrated in experiments [19].

In this work, we prepared the $\text{Mo}_{0.5}\text{W}_{0.5}\text{S}_2$ and presented a $\text{Mo}_{0.5}\text{W}_{0.5}\text{S}_2$ SA based Q-switched fiber laser at 1560 nm at the first time. Two different types of SAs including fiber-tapered $\text{Mo}_{0.5}\text{W}_{0.5}\text{S}_2$ SA and $\text{Mo}_{0.5}\text{W}_{0.5}\text{S}_2$ -PVA thin film are proposed to achieve Q-switching mechanism. With $\text{Mo}_{0.5}\text{W}_{0.5}\text{S}_2$ depositing on the surface of the tapered fiber, a minimum pulse duration of 1.42 μs and a maximum single pulse energy of 172.9 nJ are obtained. While transferring $\text{Mo}_{0.5}\text{W}_{0.5}\text{S}_2$ onto fiber end face, which is sandwiched in the fiber cavity, a maximum single pulse energy of 246.5 nJ is achieved, and the minimum pulse duration obtained is 1.92 μs . The modulation depth of $\text{Mo}_{0.5}\text{W}_{0.5}\text{S}_2$ film measured by nonlinear saturable absorption experiment is 15%.

2. Material preparation and characterization

The $\text{Mo}_{0.5}\text{W}_{0.5}\text{S}_2$, MoS_2 , and WS_2 are manufactured by microwave-assisted solvothermal method [20]. In Fig. 1, θ represents the angle between the diffraction X-ray and the certain crystal plane of the sample. The diffraction peaks of the $\text{Mo}_{0.5}\text{W}_{0.5}\text{S}_2$ crystal have three broad peaks at around $2\theta = 14.7^\circ$, 33.1° and 58.8° corresponding respectively to the (002), (100), and (110) planes of the hexagonal $\text{Mo}_{0.5}\text{W}_{0.5}\text{S}_2$, which indicates the partly crystalline in the sample, which is attributed to the limitation of the preparation method in the experiment. Figure 1(b) shows the scanning electron microscope (SEM) image of the $\text{Mo}_{0.5}\text{W}_{0.5}\text{S}_2$.

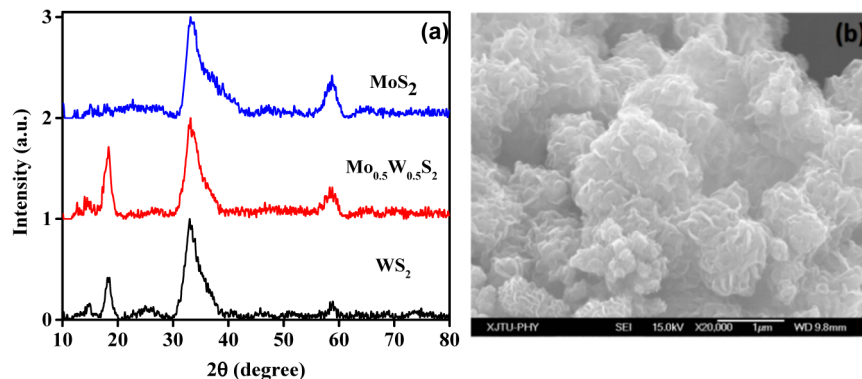


Fig. 1. (a) The X-ray diffraction (XRD) pattern of $\text{Mo}_{0.5}\text{W}_{0.5}\text{S}_2$. (b) The SEM image of $\text{Mo}_{0.5}\text{W}_{0.5}\text{S}_2$.

In the experiment, two different types of $\text{Mo}_{0.5}\text{W}_{0.5}\text{S}_2$ are prepared to obtain passive Q-switching. The first one is realized by interaction between the $\text{Mo}_{0.5}\text{W}_{0.5}\text{S}_2$ and the evanescent wave of the taper fiber. The fabrication method of fiber taper is similar to previous report [21], which is fabricated by the flame brushing technique with SMF28. Figure 2(b) shows the sketch of taper fiber, the length of the fiber-taper is 25 mm (including transition region and taper waist), and the waist is 2 μm . we put the tapered fiber on U-type groove and insert them into quartz capillary. The $\text{Mo}_{0.5}\text{W}_{0.5}\text{S}_2$ -alcohol solution is injected into the quartz tube to deposit the SA on the fiber taper. Then two end sides of quartz capillary are sealed by ultraviolet (UV) curing adhesive to prevent SA from the ambient. Figure 2(a) shows the encapsulated taper fiber, and Fig. 2(c) is a schematic diagram of fiber taper viewed by a microscope equipped with a microscope objective with magnification $\times 100$. The second type of SA is based on $\text{Mo}_{0.5}\text{W}_{0.5}\text{S}_2$ -PVA film, which fabrication process can be described as follows. First, the prepared $\text{Mo}_{0.5}\text{W}_{0.5}\text{S}_2$ powder is dissolved in N-Methyl pyrrolidone (NMP) solution with a concentration of $\sim 1.25\text{mg/ml}$, then mixed by a magnetic stirrer for 1 hour, and ultrasonicated for 2 hours. The medical PVA powder is dissolved in deionized water with a concentration of $\sim 5\%$ wt. Third, The mixture of the $\text{Mo}_{0.5}\text{W}_{0.5}\text{S}_2$ solution and PVA solution is ultrasonicated for 2 hours to ensure the $\text{Mo}_{0.5}\text{W}_{0.5}\text{S}_2$ homogeneously distributed in the PVA solution. At last, evaporating the mixture at room temperature on a culture ware, then it will formed into a filmy PVA- $\text{Mo}_{0.5}\text{W}_{0.5}\text{S}_2$ composite. In the experiment, $\text{Mo}_{0.5}\text{W}_{0.5}\text{S}_2$ -PVA film is cut into $1\text{mm}\times 1\text{mm}$ and transferred onto the end face of fiber and sandwiched between two fiber flanges to achieve Q-switching operation.

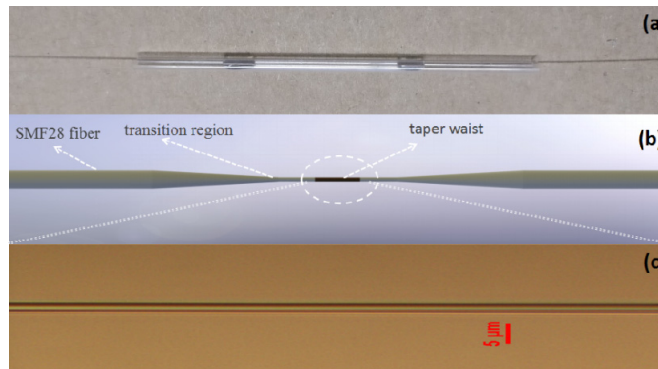


Fig. 2. (a) Image of the encapsulated taper fiber. (b) The sketch of tapered fiber. (c) Image of the taper waist under $1000\times$ microscope.

For SAs, the nonlinear absorption property is an indispensable characterize the optical properties of materials. So we build a twin-detector system to measure nonlinear transmission of SA. The illuminant is a home-made Er-doped Nonlinear Polarization Evolution (NPE) mode-locking fiber laser with the repetition of 52. 16 MHz, pulse duration of 300 fs, center wavelength of 1560 nm. The measured results and fitted curve with the following formula is shown as Fig. 3.

$$T(I) = 1 - \Delta T \times \exp(-I / I_{sat}) - A_{ns}$$

where T , ΔT , I , I_{sat} , A_{ns} represent transmittance, modulation depth, laser intensity, saturation power intensity and non-saturable absorbance, respectively. From the Fig. 3(b), the modulation depth of the $\text{Mo}_{0.5}\text{W}_{0.5}\text{S}_2$ -PVA film is evaluated to be 15%. The saturating intensity and non-saturable loss is about 13.97MW/cm^2 and 30%, respectively.

3. Experimental setup and results

All-fiber lasers have a lot of advantages such as tight configuration, reliable performance, low environmental impact over solid-state lasers, and providing a convenient platform to measure

nonlinear absorption of various kinds of samples. Figure 3(a) shows the experimental equipment of the Er-doped passively Q-switching oscillator, which consists of a 29 cm long highly doped Erbium fiber(Liekki Er-110-4/125), a wavelength-division multiplexer, an optical coupler with output rate of 20%, a $\text{Mo}_{0.5}\text{W}_{0.5}\text{S}_2$ SA, a polarization independent isolator, and a polarization controller. The ring cavity is pumped by a diode laser with a central wavelength of 976 nm. Highly doped Erbium fiber is used as gain medium to provide gain of cavity, the polarization independent isolator and polarization controller are used to ensure the unidirectional transmission of light and to adjust the polarization of beam. The total length of the cavity is 3.78 m.

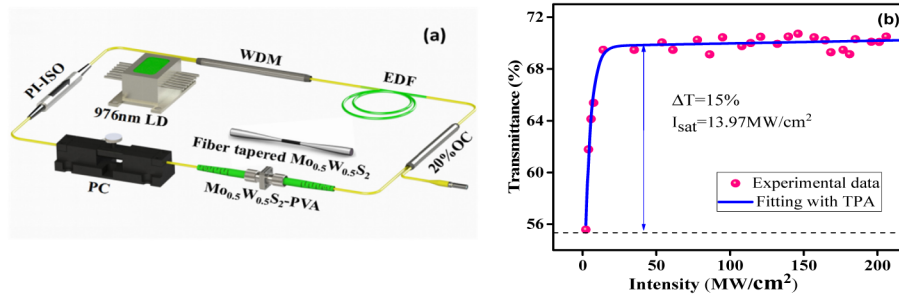


Fig. 3. (a) Diagram of the Er-doped Q-switched fiber setup with fiber tapered and PVA of $\text{Mo}_{0.5}\text{W}_{0.5}\text{S}_2$ SA (b) Nonlinear absorption of $\text{Mo}_{0.5}\text{W}_{0.5}\text{S}_2$ -PVA film.

We use oscilloscope to observe the output pulse from the cavity. Figure 4(a) and Fig. 4(b) depict a series of stable pulse trains of PVA film SA and fiber tapered SA under different pump power, respectively. For $\text{Mo}_{0.5}\text{W}_{0.5}\text{S}_2$ -PVA film, a stable Q-switching mechanism appears when pump power is set as 180 mW. While for fiber tapered one, the Q-switching threshold decreased to 140 mW at the same condition. The result indicates that fiber tapered SA is easier to achieve Q-switching threshold due to the interaction between evanescent field of the taper fiber and SAs. Figure 5 shows the shortest pulse duration of this two types of $\text{Mo}_{0.5}\text{W}_{0.5}\text{S}_2$ -based Erbium doped fiber oscillator. Figure 5(a) presents the single pulse of $\text{Mo}_{0.5}\text{W}_{0.5}\text{S}_2$ -PVA film based mechanism when pump power is 460 mW, and Fig. 5(b) presents the pulse of fiber tapered SA with pump power of 550 mW. It can be noted that Q-switching pulse with fiber tapered SA possesses a shorter duration of 1.42 μs than 1.92 μs of PVA film SA, which is due to the tapered fiber own a long interaction distance between evanescent wave and $\text{Mo}_{0.5}\text{W}_{0.5}\text{S}_2$. Pulse duration is closely related to the modulation depth according to [22]. From the reference [23], a long interaction between evanescent wave and SA will also increase the modulation depth. So we deduce that fiber tapered SA may own a larger modulation depth than the film one.

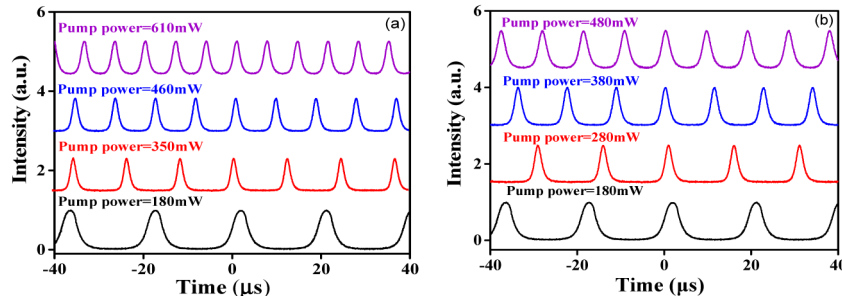


Fig. 4. The various pulse trains of (a) $\text{Mo}_{0.5}\text{W}_{0.5}\text{S}_2$ -PVA film and (b) fiber tapered $\text{Mo}_{0.5}\text{W}_{0.5}\text{S}_2$ obtained under different pump powers.

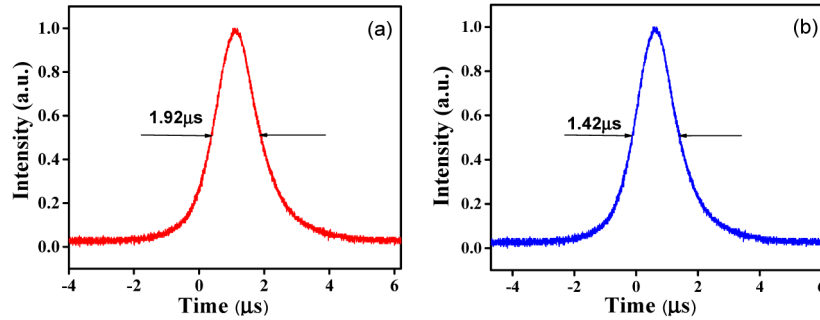


Fig. 5. The single pulse profile of (a) $\text{Mo}_{0.5}\text{W}_{0.5}\text{S}_2$ -PVA film and (b) fiber tapered $\text{Mo}_{0.5}\text{W}_{0.5}\text{S}_2$.

Figure 6 depicts the evolution of pulse duration and repetition rate varies with the pump power. Figure 6(a) shows the repetition rate of $\text{Mo}_{0.5}\text{W}_{0.5}\text{S}_2$ -PVA film increasing from 52 kHz to 118.4 kHz, and pulse duration goes down from 3.42 μs to 1.95 μs and then floating nearby 2 μs with the increasing of pump power, which may be attributed to the thermal influence to $\text{Mo}_{0.5}\text{W}_{0.5}\text{S}_2$ -PVA film. Comparing to fiber tapered one, the thin film SA quickly obtains the minimum pulse duration than fiber tapered SA does. This is due to the high intensity at fiber coupling, while the intensity of the evanescent field is quite low, but the interaction length of the evanescent field with the SA is longer. Figure 6(b) shows the repetition rate of fiber tapered $\text{Mo}_{0.5}\text{W}_{0.5}\text{S}_2$ SA increasing from 34.1 kHz to 98.5 kHz, corresponding to the pulse durations decrease from 4.72 μs to 1.42 μs with the improvement of pump power. Different to mode-locking, the repetition are related to pump power but not cavity length, which meet the characteristics of Q-switching system. It also shows that the fiber laser with fiber tapered SA outputs a higher repetition rate and a narrower pulse duration under the same pump power.

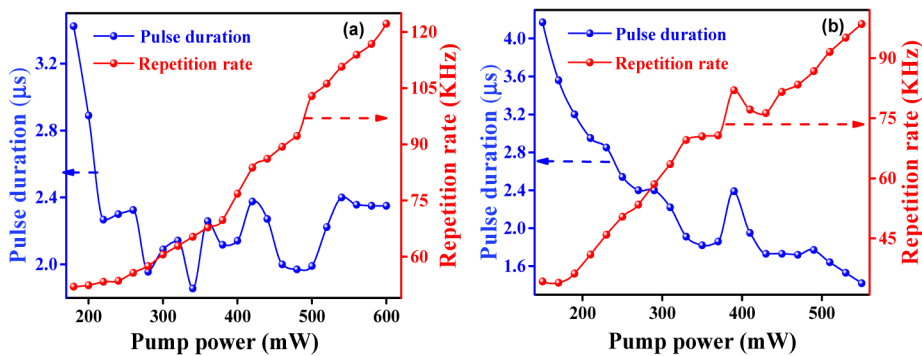


Fig. 6. Pulse duration and repetition rate versus incident pump power of (a) $\text{Mo}_{0.5}\text{W}_{0.5}\text{S}_2$ -PVA film and (b) fiber tapered $\text{Mo}_{0.5}\text{W}_{0.5}\text{S}_2$.

It can be seen in Fig. 7, when the pump power raises, the output power the pulse energy goes up at first and then goes down, but the Q-switching exits all the time, when the pump power increases, the repetition rate of output pulse simultaneously increases and the pulse duration decreases monotonically. Which are typical features of Q-switching pulse trains. The maximum pulse energy of $\text{Mo}_{0.5}\text{W}_{0.5}\text{S}_2$ -PVA film we can see in Fig. 7(a) is 246.5 nJ, which is higher than fiber tapered one of 172.9 nJ in Fig. 7(b). Although the thin diameter of taper fiber can enhance the interaction between the evanescent field and the SA on the fiber surface, it also results in higher loss in the fiber cavity. Therefore, it is of great importance to make the tapered fiber with appropriate waist diameter to achieve higher energy and narrower pulse duration. The average output power of this two types of SA increases linearly with the improvement of incident power. The maximum output power of $\text{Mo}_{0.5}\text{W}_{0.5}\text{S}_2$ -PVA film is 26.9 mW with the incident power varying in the range of 180 mW to 610 mW. While the

maximum output power of fiber tapered $\text{Mo}_{0.5}\text{W}_{0.5}\text{S}_2$ is 15.6 mW with the incident power varying from 140 mW to 550 mW. When the pump power is higher than 550 mW, the pulse train become unstable and even disappear. However when one decrease the pump power, the Q-switching appears again, this phenomenon is attributed to the over-saturation rather than the thermal damage of SAs [24]. We compare the other reports with our results about passively Q-switching fiber laser based on pure MoS_2 and WS_2 at 1.5 μm wavelength. As Table 1 shows, $\text{Mo}_{0.5}\text{W}_{0.5}\text{S}_2$ SA based Q-switching fiber laser in this work achieved highest pulse energy both on PVA film SA and fiber tapered SA compared with this two types pure MoS_2 and WS_2 SAs.

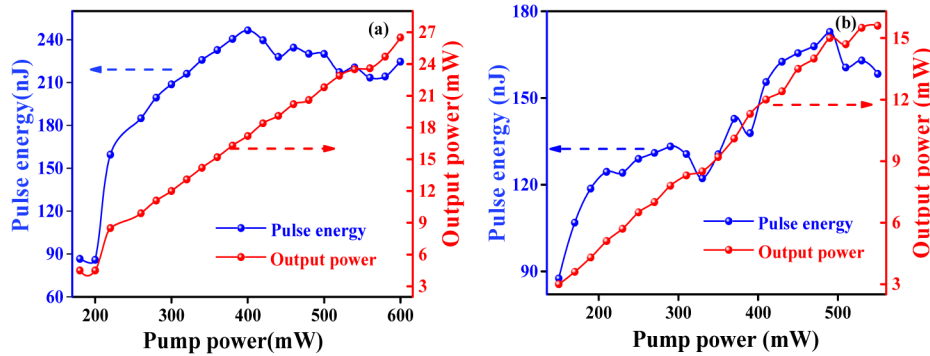


Fig. 7. Output average power and pulse energy versus incident pump power of (a) $\text{Mo}_{0.5}\text{W}_{0.5}\text{S}_2$ -PVA film and (b) fiber tapered $\text{Mo}_{0.5}\text{W}_{0.5}\text{S}_2$

Table 1. Typical Q-switched fiber laser at 1.5 μm wave band.

Year	SA	Repetition rate(KHz)	Pulse duration (μs)	Pulse energy (nJ)	Modulation depth	Wavelength (nm)	Ref.
2013	MoS_2 film	10.6-173.1	1.66	27.2	33.2%	1549.9	[25]
2014	MoS_2 -SAM	116-131	0.66	152	9%	1549.8	[26]
2015	MoS_2 -PVA	28.6-114.8	1.92	8.2	28.5%	1560.5	[27]
2015	MoS_2 -PVA	7.76-41.45	12.9	184.7	2.15%	1560	[28]
2015	Fiber side polished WS_2	82-134	0.71	19		1567.8	[29]
2015	Fiber tapered WS_2	33-108	1.3	72		1565	[30]
2015	WS_2 -PVA	79-97	1.1	179.6	4.9%	1558	[31]
2016	MoS_2 -PVA	30.1-64.8	1.9	51.84	53.4%	1560	[32]
2016	WS_2 -SAM	29.5-367.8	0.0685	68.5	7.7%	1560	[33]
2017	WS_2 -PVA	16.1-60.9	2.376	195	2%	1565	[34]
2017	$\text{Mo}_{0.5}\text{W}_{0.5}\text{S}_2$ -PVA	52-118.4	1.92	246.5	15%	1560	This Work
2017	Fiber tapered $\text{Mo}_{0.5}\text{W}_{0.5}\text{S}_2$	34.15-98.5	1.42	168		1560	This Work

We measured the wavelength of the output pulse trains based on two types of SAs. Figure 8(a) presents the central wavelength of $\text{Mo}_{0.5}\text{W}_{0.5}\text{S}_2$ -PVA film SA is 1560.8 nm with an optical spectrum bandwidth of 5 nm. As for fiber tapered SA, Fig. 8(b) shows a central wavelength of 1555.5 nm with an optical spectrum of 5.33 nm. When pump power increases to 500 mW, a central wavelength of 1530 nm emerges as the inset of Fig. 8(b), which is due to the combination of the high nonlinear effect of the $\text{Mo}_{0.5}\text{W}_{0.5}\text{S}_2$ -based fiber taper and the spectral filtering effect induced by the birefringence in the cavity [35].

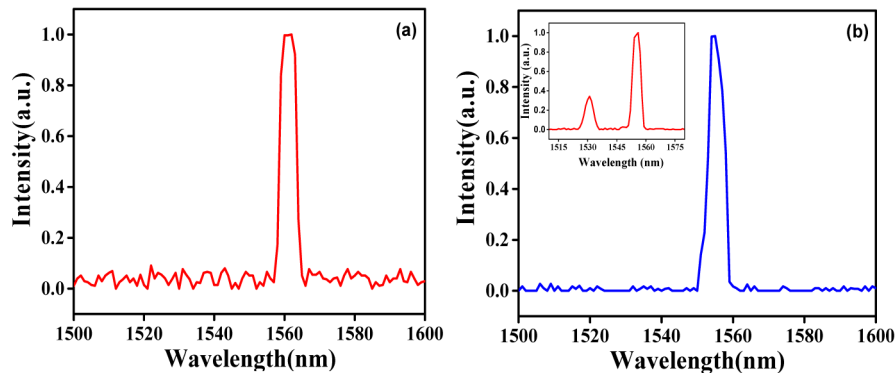


Fig. 8. The wavelength spectrum of Q-switched Er-doped fiber based on (a) $\text{Mo}_{0.5}\text{W}_{0.5}\text{S}_2$ -PVA film and (b) fiber tapered $\text{Mo}_{0.5}\text{W}_{0.5}\text{S}_2$, inset shows the dual-wavelength mechanism.

4. Conclusion

In conclusion, a stable passively Q-switching fiber laser based on two types of $\text{Mo}_{0.5}\text{W}_{0.5}\text{S}_2$ SAs (the $\text{Mo}_{0.5}\text{W}_{0.5}\text{S}_2$ -PVA film and fiber tapered $\text{Mo}_{0.5}\text{W}_{0.5}\text{S}_2$) was demonstrated. Comparing this two types of SA, it can be revealed that the $\text{Mo}_{0.5}\text{W}_{0.5}\text{S}_2$ -PVA film-based Q-switching operation possesses a higher pulse energy and a higher average output power, while fiber tapered Q-switching operation with $\text{Mo}_{0.5}\text{W}_{0.5}\text{S}_2$ SA own a shorter pulse duration and lower Q-switching threshold. In addition, it shows that $\text{Mo}_{0.5}\text{W}_{0.5}\text{S}_2$ possesses a high modulation of 15%. The experimental results obviously show that $\text{Mo}_{0.5}\text{W}_{0.5}\text{S}_2$ can be considered as a promising candidate for fiber laser applications and other photoelectric device.

Funding

National Natural Science Foundation of China (NSFC) (61675158); Fundamental Research Funds for the Central Universities (JBG160504).